ASIAN JOURNAL OF PHARMACEUTICAL AND CLINICAL RESEARCH

INNOVARE ACADEMIC SCIENCES
Knowledge to Innovation

Vol 18, Issue 4, 2025

Online - 2455-3891
Print - 0974-2441

Research Article

INVESTIGATING THE ANTI-CANCER PROPERTIES OF A NEWLY SYNTHESIZED METAL-QUERCETIN NANOCOMPLEX IN THE CONTEXT OF CERVICAL CANCER

SHUBHAM KAMBLE[1]*, GOVIND K LOHIYA[2], PRIYANKA SHARNANGAT[3], MONIKA KHERADE[4], TIRUPATI RASALA[1], JANHAVI INDURKAR[5], AKSHAY RAMTEKE[2]

[1]Department of Pharmaceutics, The Royal Gondwana College of Pharmacy, Nagpur, Maharashtra, India. [2]Department of Pharmaceutics, Gurunanak College of Pharmacy, Nagpur, Maharashtra, India. [3]Department of Quality Assurance, Gurunanak College of Pharmacy, Nagpur, Maharashtra, India. [4]Department of Pharmacognosy, The Royal Gondwana College of Pharmacy, Nagpur, Maharashtra, India. [5]Department of Pharmaceutical Chemistry, Gurunanak College of Pharmacy, Nagpur, Maharashtra, India.
***Corresponding author: Shubham Kamble; Email: shubhkamble121@gmail.com**

Received: 12 January 2025, Revised and Accepted: 20 March 2025

ABSTRACT

Objectives: This study aims to develop and evaluate quercetin-loaded silver nanoparticles (Q-AgNPs) as a potential therapeutic agent against cervical cancer, assessing their cytotoxic effects on HeLa cell lines.

Methods: Quercetin was synthesized into AgNPs using a bioreduction method involving silver nitrate, with subsequent characterization performed using ultraviolet (UV)-Visible spectroscopy, Fourier Transform Infrared spectroscopy, X-ray diffraction, and scanning electron microscopy. The cytotoxicity of Q-AgNPs was evaluated *in vitro* on HeLa cervical cancer cells using the MTT assay to determine cell viability and calculate the IC_{50} value.

Results: The characterization of Q-AgNPs revealed successful synthesis, with distinctive peaks observed in UV-Visible spectroscopy confirming the interaction between quercetin and silver. The particle size analysis indicated a range of sizes, with an entrapment efficiency of 85.4%. The cytotoxicity assessment demonstrated a dose-dependent decrease in HeLa cell viability, with an IC_{50} value calculated at 11.765 µg/mL, indicating significant cytotoxic effects.

Conclusion: The findings highlight the promising potential of Q-AgNPs as an innovative approach for cervical cancer therapy. Further optimization and *in vivo* studies are warranted to explore the mechanisms of action and enhance the therapeutic efficacy of this nanoparticle formulation.

Keywords: Quercetin, Silver nanoparticle, Anticancer, Hela, cell line, Scanning electron microscopy-energy dispersive X-ray.

 DOI: http://dx.doi.org/10.22159/ajpcr.2025v18i4.53670. Journal homepage: https://innovareacademics.in/journals/index.php/ajpcr

INTRODUCTION

Carcinoma of uterine cervix (CC) is having a devastating effect on women's health around the world, especially in developing countries with an estimated rate of 527,624 new cases and 265,672 deaths per year. It ranks as the second most common cancer worldwide in occurrence and the leading cause of death among women in developing countries. In 99.5% of CC, high-risk human papilloma virus types 16, 18, 31, and 33 infections had a major role in tumor development [1,2]. Cervical cancer is often initially treated with surgery to remove the cancer [3,4]. Additional treatments may involve medications designed to destroy cancer cells [5,6]. Quercetin (Qu) is an essential phytoconstituent that acts as a building block for many other flavonoids [7,8]. This unique flavonoid is present in a wide range of vegetables and fruits, including onions, berries, apples, tea, and brassicas, as well as in various seeds, flowers, nuts, barks, leaves, and medicinal plants such as *Ginkgo biloba*, *Piper cubeba*, *Solanum trilobatum*, and *Withania somnifera* [9]. Quercetin, a type of flavonoid, is a compound that you can find naturally in many foods, particularly in fruits and vegetables. It is especially plentiful in onions, buckwheat, and broccoli [10]. Due to its health benefits, quercetin is often added to functional foods and sold as a dietary supplement [11]. There is ongoing research into its potential role in preventing or treating various diseases, including some forms of cancer. Research on nanomaterials (NMs) began in the late 20th century, with silver nanoparticles (AgNPs) emerging as a key innovation [12,13]. These nanoparticles are utilized in numerous fields, including healthcare, food safety, agriculture, environmental applications, biomedical technologies, and catalysis [14]. These nanoparticles exhibit superior stability, water solubility, non-toxicity, and biocompatibility compared to organic materials [15]. In this context, the most practical and effective nanoparticles were identified to be within the 1–100 nm range, all of which were produced using chemical methods. Many nanoparticles, such as ZnO, FeO, SiO_2, CeO_2, and TiO_2, are commonly utilized for their favorable photocatalytic properties [16]. In addition, elemental metals such as Ag, Au, Fe, Cu, Pt, Pd, Ni, and Co, when in nanometric sizes, are extensively used for various applications, including antimicrobial effects, optical properties, catalysis, antioxidant activities, and anticancer treatments [16]. AgNPs are highly effective in antibacterial applications because of their strong, broad-spectrum activity, and minimal development of resistance [17,18]. Their effectiveness is further increased when used in combination with antibiotics. Green synthesis methods, which utilize natural sources and environmentally friendly processes, provide a convenient way to produce AgNPs [19,20]. These approaches not only reduce energy consumption and lower costs but also yield biocompatible NMs with controlled properties [13,21,22]. This makes AgNPs a sustainable and effective option for antibacterial applications in fields such as biomedicine and environmental remediation, while aligning with eco-friendly and cost-efficient practices [23]. AgNPs can be produced through various methods, including chemical, physical, and biological approaches. One notable advantage of physical techniques is their ability to achieve a more uniform size distribution compared to chemical methods. However, a key drawback of physical methods is their high energy consumption [24]. This research presents a novel method for producing Qu-loaded AgNP (Q-AgNPs) that incorporate unique elements. It investigates the effects of Qu derivatives on the stability and anticancer properties of the nanoparticles while also developing

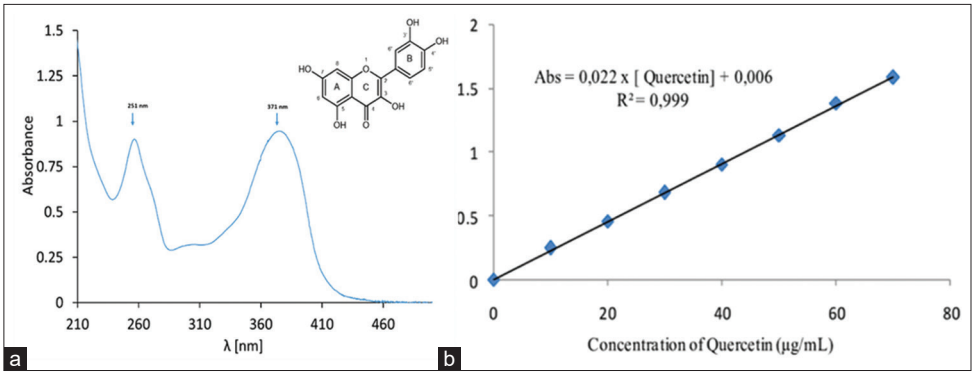

Fig. 1: (a) Lamda max, (b) Calibration curve of quercetin API

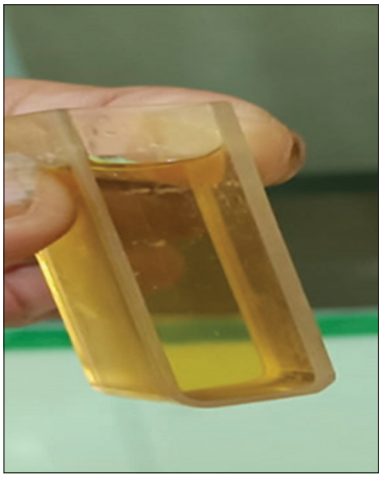

Fig. 2: Prepared silver nano evidenced by the appearance of brown color

a biocompatible coating. In addition, the study offers insights at the molecular level and examines safety concerns through cell line studies, particularly focusing on lower IC_{50} values. These features set it apart from previous research in the field.

MATERIALS AND METHODS

Material

The Qu (98% pure) was purchased from Yarrow Chem Products, Mumbai, Maharashtra, India. Silver nitrate was purchased from Thermo Fisher Scientific Private Limited., Mumbai, India, Other chemicals, including trisodium citrate, were procured from Nice Chemicals Private Limited, Mumbai, India. Methanol was obtained from Loba Chemie Private Limited, Mumbai, India, HeLa cell line procured from NCCS Pune, Maharashtra, India and other solvents and chemicals employed were of analytical grade.

Organoleptic characteristics

Visual observations were conducted to assess various organoleptic properties, including general appearance, color, texture, and odor, to identify the medication [25]. For color analysis, a small drug sample was placed on butter paper and examined under good lighting conditions. To evaluate the odor, a small quantity of the drug was sniffed to capture its fragrance.

Detection of melting point

The melting point was measured using the USP method. A small sample of the medication was placed in a sealed capillary tube, which was then inserted into the melting point apparatus. The temperature of the device was gradually increased, and observations were made to determine the temperature at which the medication started to melt, as well as the temperature at which it completely melted [26].

Dual scanning calorimetry (DSC)

The DSC TA 60 Shimadzu thermal analyzer was used for the DSC tests. High-purity indium metal was employed for instrument calibration. The scans were conducted in a nitrogen atmosphere, with a heating rate set at 10°C/min [26].

Spectroscopy used for ultraviolet (UV)-visible analysis

Identifying the wavelengths of Qu

We use a UV-Vis spectrophotometer with a 1 cm quartz cuvette to identify the Qu wavelengths. Qu is dissolved in a suitable solvent such as water or ethanol at a standard concentration under experimental conditions. The wavelength range measured is between 200 and 800 nm, with baseline correction applied, and readings taken at room temperature. UV-Vis spectrophotometers typically scan at a standard speed of 200 nm/min [27].

Establishing the ethanol standard curve

10 mg of quercetin (dihydrate) was dissolved in 10 mL of methanol to prepare a 100 µg/mL stock solution. The solution was filtered, and the spectrum was recorded from 400 to 200 nm using methanol as the blank. From the stock solution, different working standard solutions were prepared by pipetting out 0.5 mL, 1 mL, 1.5 mL, 2 mL, and 2.5 mL into separate 10 mL volumetric flasks, and the volume was made up with methanol. The λmax was determined by scanning the samples in the range of 400–200 nm, and the absorbance values of the working standard solutions were noted at 372 nm [27].

AgNP synthesis-selection of appropriate metal for complex

The selection of an appropriate metal for quercetin metal nanoparticles was based on several factors. Quercetin was known to interact with metal ions to form metal-quercetin complexes, which could be utilized for the synthesis of metal nanoparticles [28]. The selection of the appropriate metal was guided by the ability of the metal to form stable complexes with quercetin, the potential for enhanced biological activities, and the ease of nanoparticle synthesis. Common metals that had been explored for the synthesis of quercetin metal nanoparticles included silver (Ag) and gold (Au). These metals had shown the ability to form stable complexes with quercetin and exhibited promising biological properties [29].

Synthesis of Qu-AgNP

A stock solution of quercetin was prepared at a concentration of 2 mM (60 mg in 100 mL) using a 1 mM (0.004 mg in 100 mL) sodium hydroxide solution. The quercetin stock solution was stored at room temperature. Next, 1 mM of 10 mL silver nitrate was prepared, to which 0.1 mL of quercetin solution was added in a drop-wise manner under constant stirring at room temperature. This facilitated the bioreduction of silver ions (Ag+) to neutral ions (Ag0) in the solution, which was evidenced by the appearance of brown color [30]. The resultant colloidal AgNPs were filtered through a 0.22-micron Nylon syringe filter, centrifuged the filtered solution using cooling centrifuge

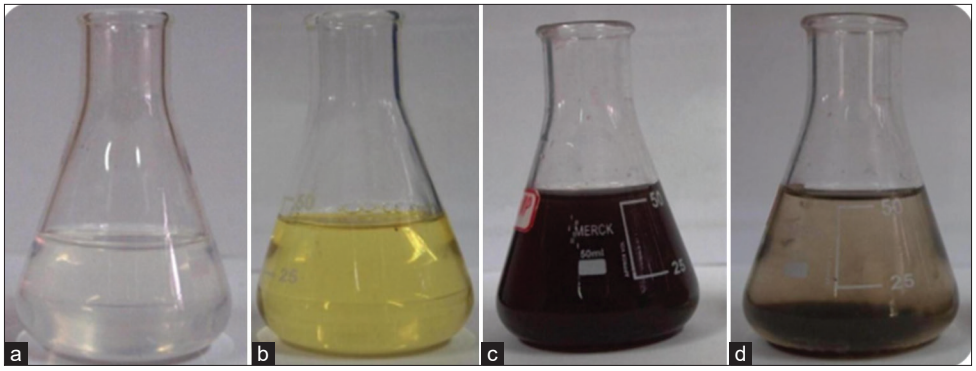

Fig. 3: Physical appearance of silver nitrate, quercetin in NaoH, Qu-silver nanoparticle, sediment nanoparticle as a,b,c,d respectively

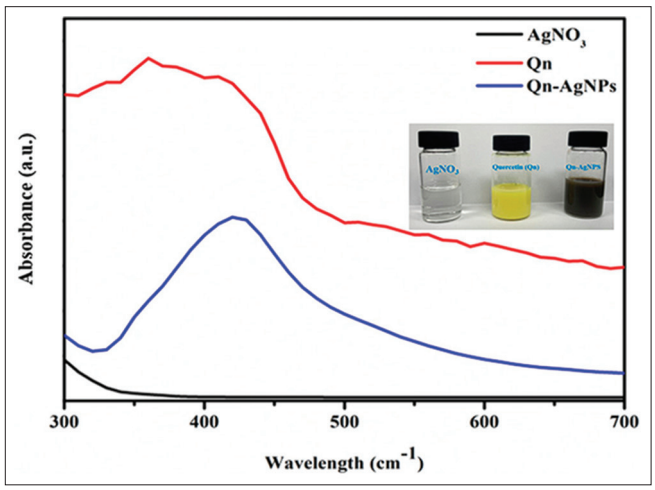

Fig. 4: Ultraviolet-visible spectrum of $AgNO_3$, quercetin, quercetin-loaded silver nanoparticles

at 15,000 rpm for 20 min., separated the sediment in Chine dish, and Dried at 65°C for 16 h.

Nanoparticles evaluation

Effective drug trapping

The composition of the nanoparticle suspension was assessed through a series of measurements. Initially, 5 mL of this formulation was diluted with distilled water to reach a total volume of 8 mL. The separation of components was achieved using a high-speed centrifuge (Remi Private Limited, Maharashtra, India). The centrifugation process was carried out for 45 min at an impressive speed of 30,000 rpm, with the cooling system active to maintain optimal conditions. After centrifugation, the resulting mixture underwent phase separation, yielding a supernatant and sediment. The volumes of both fractions were carefully calculated. Subsequently, the sediment was lysed utilizing n-propanol and then passed through a 0.4 µm nylon disk filter to further purify the sample. The final step involved the quantification of Qu content in both the supernatant and sediment. This was accomplished by employing a UV spectrophotometer, with measurements taken at a specific wavelength of 420 nm, allowing for the precise determination of Qu concentrations in each fraction [31].

$$Percentage\,entrapment\,efficiency = \frac{Amount\,of\,drug\,recovered}{Total\,Amount\,of\,Drug} \times 100$$

Shape and surface morphology of nanoparticles

We analyzed the size and shape of the produced AgNPs using a scanning electron microscope (Carl Zeiss EVO 18) with an acceleration voltage of 20 kV. The nanoparticle solution was diluted 5 times using deionized water. A small amount of dispersed AgNPs was then placed on an aluminum stub and air-dried at 60°C for 5 min. Afterward, the sample was scanned, and images were taken using a photomicrograph [32].

Table 1: Solubility of drug

S. No.	Solvent	Inference
1	Methanol	Very Soluble
2	DMSO	Soluble
3	IPA	Slightly Soluble
4	Distilled Water	Not Soluble

Table 2: Interpretation of Fourier transform infrared

Function groups	Quercetin	Q-AgNPs
O–H stretch	3330.17	3300.20
C–H stretch	2922.16	2976.16
C=C stretch	1618.28	1618.28
C=O stretch	1363.67	1363.67
C-O stretch	1093.64	--
C-N stretch	1101.35	1170.79

Particle size analysis

The size of the nanoparticles was measured using the dynamic light scattering (DLS) method with the Malvern Zetasizer Nano-ZS and DTS nano software (version 6.34). To prepare for the measurements, the nanoparticle solution was diluted with distilled water, and Zetasizer cuvettes were used. Measurements were taken at 25°C, with each sample being equilibrated for at least 3 min before the readings. DLS measurements were performed during cycles of alternating increasing and decreasing temperatures. The Z-average value obtained from DLS represents the average hydrodynamic diameter of the nanoparticles. Data were collected to gain a clearer understanding of the vesicle size and size distribution [33].

Measuring zeta potential

Zeta potential, measured using a Zetasizer-1000HS (Malvern Instruments, Malvern, UK), reflects the overall surface charge of nanoparticles. In this study, a suspension was created by diluting 50 mL of double-distilled water with 5 mL of an electrolyte solution of NaCl at a concentration of 2×10^{-2} M. The pH of this suspension was then adjusted to the target level. After allowing the samples to sit for 30 min, they were agitated, and the equilibrium pH was measured to determine the zeta potential of the metallic particles. The zeta potential values were used to calculate the surface potential of AgNPs. For each condition assessed, the average of three measurements was recorded. The stability of the nanoparticles was evaluated based on zeta potential values, with stability indicated by values above +30 mV or below −30 mV [34].

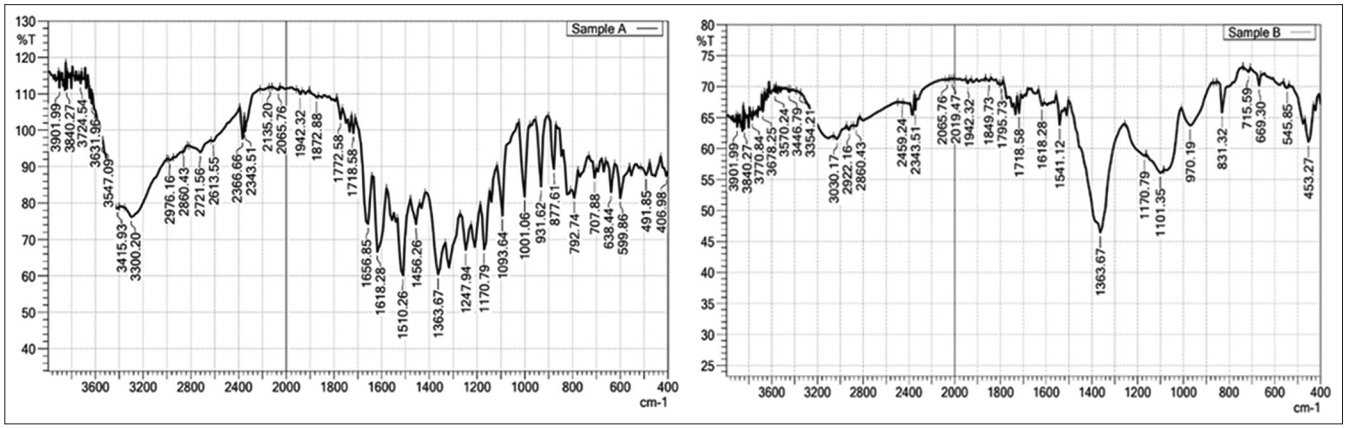

Fig. 5: Fourier transform infrared spectroscopy of quercetin-loaded silver nanoparticles and pure quercetin API

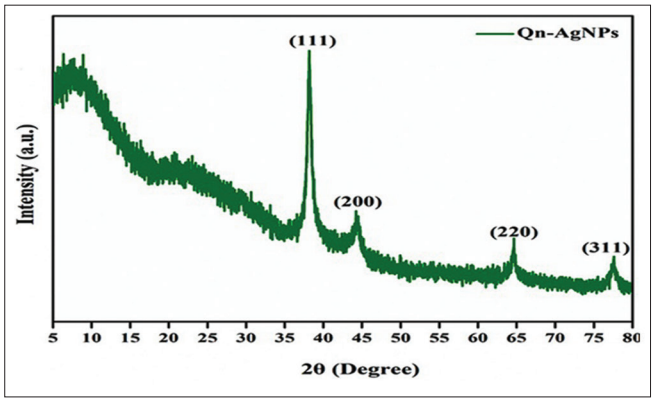

Fig. 6: X-ray diffraction of quercetin-loaded silver nanoparticles

Diffraction of X-rays

The scattering of X-rays by the atoms in a crystal generates interference patterns that provide insights into the crystal's structure or characteristics illustrated in Fig. 6. To prepare for analysis, a glass slide was coated with 1 mL of AgNP solution and then dried in an oven at 40°C. This coating process was repeated three to four times to create a thin film. X-ray diffraction (XRD) was performed using Cu K radiation (wavelengths of 1.54056 Å and 1.54439 Å) on a Philips Xpert Pro Diffractometer operating at 40 kV and 30 mA. Diffracted intensities were measured over the angle range from 35.01° to 79.99° [35].

Scanning electron microscopy (SEM)-energy-dispersive X-ray spectroscopy (EDS) analysis

SEM and SEM-energy-dispersive X-ray (EDX) were used to analyze the morphology, size, and elemental composition of nanoparticles. These techniques provide valuable insights into the nanoparticles' physical characteristics and elemental composition [36].

Cell line studies

Hela cell lines were Procure from the National Centre for Cell Sciences (NCCS), Pune, India, and cultured in Dulbecco's modified Eagle's medium (DMEM) supplemented with 10% fetal bovine serum (FBS). *In vitro* cell line, studies were carried out at CURO Biosciences Private Limited, Nagpur, Maharashtra, India.

In–vitro cell line studies

Hela cell lines were obtained from the NCCS in Pune, India, and were cultured in DMEM supplemented with 10% FBS. The cells were washed with ×1 PBS and treated with trypsin, a proteolytic enzyme, for 30 s to facilitate detachment. After shaking the flask gently for 2 min to ensure complete detachment, FBS was added to neutralize the trypsin activity, and the cells were resuspended in 10 mL of complete media. The suspension was prepared to achieve the required cell density for *in vivo* studies, with aliquots used as per the experimental setup. Silver quercetin nanoparticles were diluted in DMEM to create a 5 mg/mL stock solution, which was further diluted (1 mL in 10 ml DMEM) to the desired concentration for the study. The *in vivo* cell line experiments were conducted at CURO Biosciences Private Limited, Nagpur, India, following ethical and procedural standards.

Statistical analysis

The study on Q-AgNPs for cervical cancer therapy revealed several key statistical findings. The cytotoxicity of the nanoparticles was characterized by an IC_{50} value of 11.765 µg/mL, indicating the concentration at which 50% of HeLa cancer cells are killed. Additionally, the entrapment efficiency of quercetin within the nanoparticles was notable at 85.4%, reflecting effective drug loading. Particle size analysis showed that Batch A had an average particle size of 122.71 nm, while Batch B measured 225.5 nm, with smaller particles generally offering better cellular uptake. Furthermore, zeta potential measurements indicated that Batch A achieved a zeta potential of −31.4 mV, suggesting superior stability compared to Batch B's −24.9 mV. Together, these statistical results highlight the efficacy and potential of Q-AgNPs as promising therapeutic agents against cervical cancer.

RESULTS AND DISCUSSION

Solubility of quercetin

The solubility study of quercetin API was carried out using various solvents like methanol, IPA, DMSO, Distilled water and the results are mentioned in Table 1.

Determination of λ_{max} and calibration curve of quercetin API

In the UV–visible range of 240–500 nm, quercetin has two main absorption bands: band A (240–280 nm) and band B (340–440 nm) shown in Fig. 1.

Selection of appropriate metal for complex

AgNPs have shown significant cytotoxic effects against a range of cancer cell lines, including breast, lung, and prostate cancers. This is largely due to silver's biocompatibility and its capacity to form stable complexes, which enhance its effectiveness [35]. Moreover, combining silver with quercetin has demonstrated synergistic anticancer effects, amplifying its therapeutic potential [37]. The primary mechanisms driving these effects include inducing oxidative stress and triggering apoptosis, or programmed cell death, in cancer cells. These findings make silver-based compounds a promising avenue for developing innovative cancer treatments [38].

Formulation of metal-quercetin nano complex (MQNC) (Using silver)

A 2 mM quercetin solution was mixed with 1 mM $AgNO_3$, reducing Ag^+ to Ag^0 (brown color). The AgNPs were filtered, centrifuged (15,000 rpm, 20 min), and dried at 65°C for 16 h.

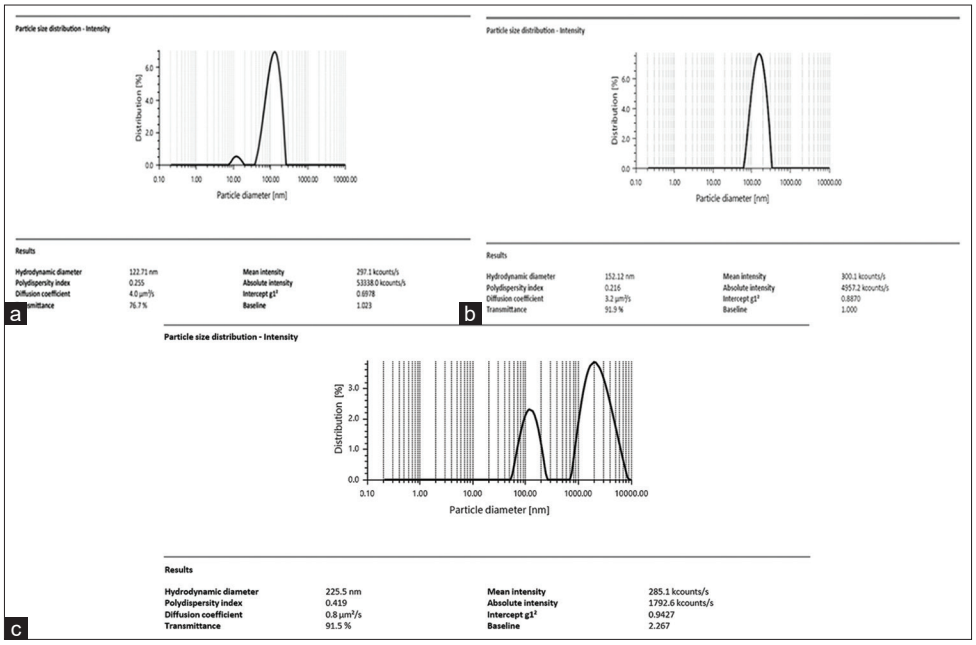

Fig. 7: Particle size analysis of batch A and B (a) Liquid Sample, (b) Solid Sample, (c) Solid sample of Batch B

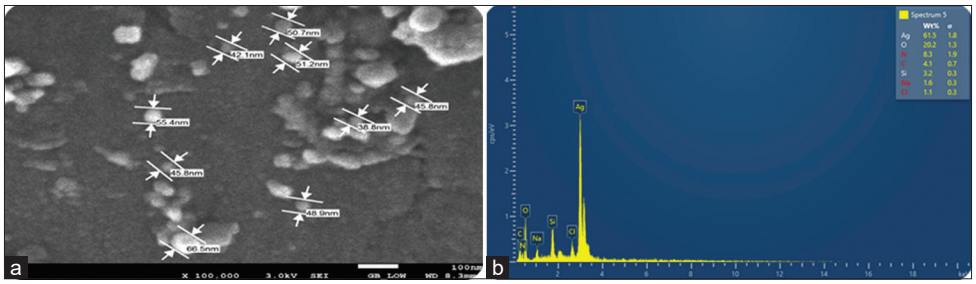

Fig. 8: Images of (a) Scanning electron microscopy (SEM) of quercetin-loaded silver nanoparticles (Q-AgNPs) and (b) SEM-energy-dispersive X-ray spectroscopy of Q-AgNPs

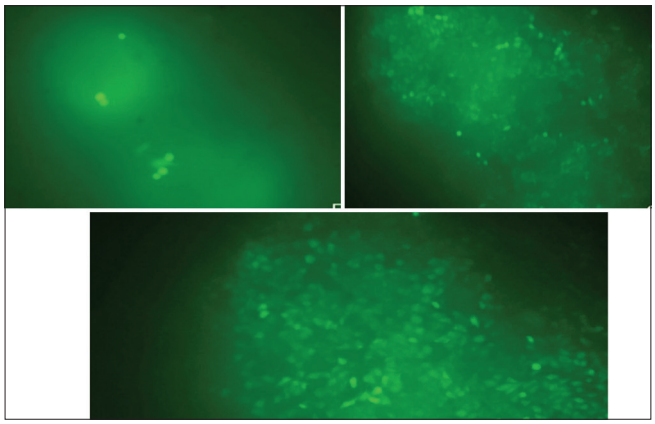

Fig. 9: Images of HeLa cells as visualized under inverted fluorescent microscope

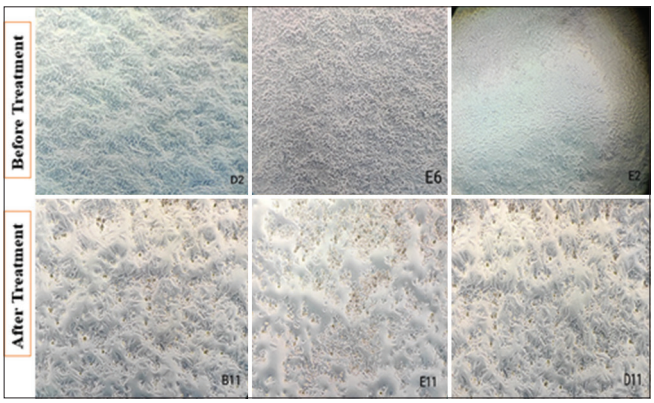

Fig. 10: Quercetin-loaded silver nanoparticles treated cell lines

Physical appearance

Its given in Figs. 2 and 3 Physical appearance of silver nitrate, quercetin in NaoH, Qu-silver nanoparticle, sediment nanoparticle as a,b,c,d respectively.

UV-Visible Spectrocopy

The UV-Visible spectrum showed distinct absorption peaks for the compounds analyzed shown in Fig. 4. Silver nitrate ($AgNO_3$) had a peak at 300 nm, while quercetin (Qu) displayed a peak at 371 nm. When quercetin was combined with silver to form nanoparticles (Qu-AgNPs), the absorption peak shifted to 424.50 nm. This red shift indicates the successful formation of quercetin-AgNPs and reflects the interaction between silver and quercetin, altering their optical properties.

Fourier transform infrared spectroscopy (FTIR)

The FTIR analysis of quercetin revealed characteristic peaks corresponding to specific functional groups is shown in Fig. 5. These included an O–H stretch at 3330.17 cm^{-1}, a C–H stretch at 2922.16 cm^{-1}, a C=C stretch at 1618.28 cm^{-1}, a C=O stretch at 1363.67 cm^{-1}, another C=O stretch at 1093.64 cm^{-1}, and a C–N stretch at 1101.35

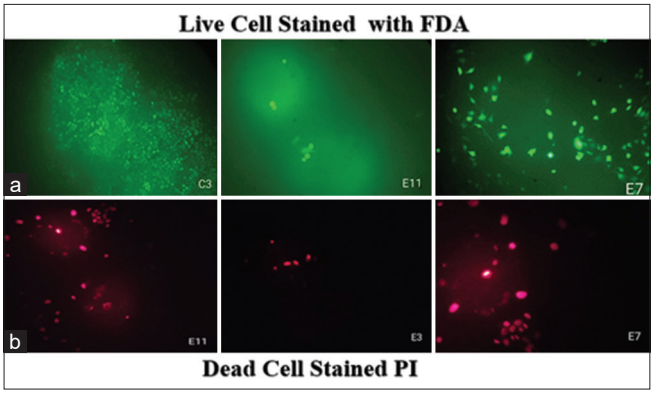

Fig. 11: Q-Ag-NC treated cell lines, (a) live cell stained with fluorescein diacetate and (b) Dead cell stained with propidium iodide

cm^{-1}. For the AgNPs synthesized with quercetin, the FTIR spectrum showed an O–H stretch at 3300.20 cm^{-1}, a C–C stretch at 2130.48 cm^{-1}, and a C=C stretch at 1618.28 cm^{-1}. In addition, a broad band in the range of 500–600 cm^{-1} was observed, which can be attributed to Ag–O vibrations, confirming the interaction between silver and quercetin in the formation of nanoparticles mentioned in Table 2.

XRD

The XRD analysis of quercetin-AgNPs (Q-AgNPs) revealed a crystalline structure. The main diffraction peaks for the AgNPs were observed at 38°, 44°, 64°, and 77° (2θ values), corresponding to the (111), (200), (220), and (311) crystal planes, respectively. These peaks confirm the crystalline nature of the AgNPs and provide evidence of their characteristic structural arrangement.

Particle size analysis

The mean particle size diameter and polydispersity indices were measured immediately after synthesis using photon correlation spectroscopy. The particle size for Batch 1 Nano Suspension was found to be 122.71 nm, while the solid sample had a particle size of 152.5 nm. For Batch 2, the solid sample had a particle size of 225.5 nm mentioned in Fig. 7. These measurements provide important insights into the size distribution and uniformity of the nanoparticles, which play a crucial role in their potential applications. Nanoparticles with a smaller size, such as the 122.71 nm particles, possess a higher surface area-to-volume ratio compared to larger nanoparticles like those measuring 225 nm. This characteristic enhances the rate of cellular uptake for smaller nanoparticles, which may also increase their potential for toxicity due to their heightened reactivity and ability to penetrate biological barriers.

Zeta potential measurements

The zeta potential value for Batch B was measured at −24.9 mV. When comparing the zeta potential values of −24 mV and −31 mV for the nanoparticles, the more negative value of −31 mV is generally considered better for nanoparticle stability. Nanoparticles with a zeta potential of −31 mV experience a higher degree of electrostatic repulsion, which promotes better colloidal stability and reduces aggregation. Based on this, Batch A, with its more negative zeta potential, is preferred for further studies. The zeta potential values for the nano suspension and solid nanoparticles ranged from −26.7 mV to −31.4 mV, indicating good stabilization and likely contributing to the narrow size distribution. Furthermore, the consistent zeta potential and size distribution of the quercetin-treated AgNPs suggest they have a low tendency to aggregate, ensuring their stability and uniformity in solution.

Entrapment efficiency

The nanoparticle suspension was prepared by adding a 10 mg sample to 10 mL of distilled water, followed by centrifugation at 12,000 rpm for 45 min. After centrifugation, the supernatant and sediment were carefully separated. The sediment was treated with n-propanol, filtered, and the quercetin (Qu) content was quantified using a UV-Visible spectrophotometer at 371 nm. This meticulous process allowed for an accurate determination of the quercetin concentration in the nanoparticle suspension, which was found to be 85.4%.

SEM-EDS analysis

The results from scanning electron microscopy (SEM) indicate that the average particle size of the synthesized nanoparticles is 52.73 nm, suggesting that they are uniform and spherical in shape, as illustrated in Fig. 8a. The purity and elemental composition of the nanoparticles were assessed using scanning electron microscopy with energy-dispersive X-ray spectroscopy (SEM-EDS). A prominent and narrow peak at 3 keV in the X-ray microanalysis confirmed the presence of silver as the primary component. Additionally, smaller peaks corresponding to elements such as O, N, C, Si, Na, and Cl are observed, as shown in Fig. 8b. The presence of silicon and chlorine in small amounts may indicate potential contamination from the environment during the synthesis, transport of the nanoparticles, or analysis of their characteristics.

Cellular uptake of Q-AgNPs

The cellular uptake, internalization, and sustained retention of nanoparticles were the important markers in therapeutic effect judgment. In this research, fluorescein diacetate and propidium iodide were used to visualize the Q-Ag-NC internalization and distribution into the HeLa cell lines, as illustrated in Fig. 9.

***In-vitro* cytotoxicity by MTT assay**

Quercetin-loaded silver nanoparticles treated cell lines are depicted in Fig. 10. The *in-vitro* cytotoxicity analysis using the MTT assay demonstrated a dose-dependent decrease in the survival of HeLa cervical cancer cells upon exposure to Q-AgNPs. At a concentration of 25 µg/mL, the percent cell survival was 34.8%, indicating a substantial cytotoxic effect. Using the formula:

$$IC_{50} = \frac{(50\% - \%cell\ survival\ at\ 25\ \mu g/ml)}{(\%cell\ survival\ at\ 25\ \mu g/ml)} \times 25\ \mu g/ml \quad (1)$$

The IC_{50} value was calculated to be 11.765 µg/mL. This indicates that the concentration required to reduce cell survival to 50% is significantly low, highlighting the potent cytotoxic effect of Q-AgNPs on HeLa cells. These findings suggest that Q-AgNPs could be a promising candidate for further investigation as a therapeutic agent against cervical cancer. For the treated cell lines, (a) live cells were stained with fluorescein diacetate, while (b) dead cells were stained with propidium iodide, illustrated in Fig. 11.

DISCUSSION

This study details a simple one-pot synthesis of silver quercetin nanoparticles, thoroughly characterized using UV-Vis spectroscopy, FTIR, XRD, and SEM-EDX, which confirmed their composition, crystalline structure, and size. The nanoparticles showed a zeta potential of −26.7 mV in suspension and −31.4 mV in solid form, with particle sizes of 122.71 nm and 152.4 nm, respectively, and an 85.4% entrapment efficiency. *In vitro* testing against HeLa cervical cancer cells revealed a significant cytotoxic effect, with an IC_{50} value of 11.765 µg/mL, suggesting their potential as a cervical cancer therapeutic agent.

CONCLUSION

The detailed characterization of Q-AgNPs, which included UV-Visible spectroscopy, FTIR, XRD, zeta potential, particle size analysis, entrapment efficiency, and SEM-EDX, provided valuable insights into the nanoparticles' physicochemical properties. The significant cytotoxic effect demonstrated against HeLa cervical cancer cells, with an IC_{50} value of 11.76 µg/mL, highlights the potential of Q-AgNPs as a promising therapeutic option for treating cervical cancer. These findings underscore the need for further research to uncover the nanoparticles' mechanisms of action, optimize their formulation, and evaluate their *in vivo* efficacy and safety, paving the way for a novel approach to combating this life-threatening disease.

AUTHOR CONTRIBUTATION

SK: Conceptualization, Investigation, Project administration, Supervision, Validation, Writing – original draft, Writing –review & editing. GL: Conceptualization, Investigation, Project administration, Supervision, Writing – original draft, Writing – review & editing. PS: Conceptualization, Investigation, Project administration, Supervision, Validation, Writing – original draft, Writing – review & editing. MK: Conceptualization, Investigation, Project administration, Supervision, Writing – original draft, Writing – review & editing. TR: Conceptualization, Investigation, Project administration, Supervision, Writing – original draft, Writing – review & editing. JI: Conceptualization, Investigation, Project administration, Supervision, Validation, Writing – original draft, Writing – review & editing. AR: Conceptualization, Investigation, Project administration, Supervision, Validation, Writing – original draft, Writing – review & editing.

CONFLICTS OF INTEREST

The authors declare no conflict of interest.

AUTHOR FUNDING

The author(s) declare that no financial support was received for the research, authorship, and/or publication of this article.

REFERENCES

1. Kabir S, Jahan SM, Nowshin S, Haque MM, Islam J. Study of chemopreventive role of paddy husk on cervical adenocarcinoma human cell line (HeLa cells). Asian J Pharm Clin Res. 2024;17(3):92-5.
2. National Cancer Institute. Cervical Cancer Treatment (PDQ®): Patient Version. Available from: https://www.cancer.gov [Last accessed on 2025 Jan 09].
3. Poddar P, Maheshwari A. Surgery for cervical cancer: Consensus and controversies. Indian J Med Res. 2021;154(2):284-92. doi: 10.4103/ijmr.IJMR_4240_20
4. Denny L, Quinn M, Sankaranarayanan R. Chapter 8: Screening for cervical cancer in developing countries. Vaccine. 2006 Aug 31;24 Suppl 3:S3/71-7. doi: 10.1016/j.vaccine.2006.05.121. PMID: 16950020.
5. Regalado Porras GO, Chávez Nogueda J, Poitevin Chacón A. Chemotherapy and molecular therapy in cervical cancer. Rep Pract Oncol Radiother. 2018;23(6):533-9. doi: 10.1016/j.rpor.2018.09.002
6. Chen L, Liu S, He Y, Yao H, Yuan Z, Yang J, *et al*. Toripalimab combined with bevacizumab plus chemotherapy as first-line treatment for refractory recurrent or metastatic cervical cancer: A single-arm, open-label, phase II study (JS001-ISS-CO214). J Gynecol Oncol. 2025;36:123-34.
7. Carrillo-Martinez EJ, Flores-Hernández FY, Salazar-Montes AM, Nario-Chaidez HF, Hernández-Ortega LD. Quercetin, a flavonoid with great pharmacological capacity. Molecules. 2024;29:1000.
8. Kim BH, Choi J, Yi E, Lee JK, Won C, Ye SK, *et al*. Relative antioxidant activities of quercetin and its structurally related substances and their effects on NF-κB/CRE/AP-1 signaling in murine macrophages. Mol Cells. 2013;35:336-42. doi: 10.1007/s10059-013-0031-z
9. Kumar R, Vijayalakshmi S, Nadanasabapathi S. Health benefits of quercetin. Defence Life Sci J. 2017;2(2):142-51.
10. Dabeek WM, Marra MV. Dietary quercetin and kaempferol: Bioavailability and potential cardiovascular-related bioactivity in humans. Nutrients. 2019;11(10):2288. doi: 10.3390/nu11102288
11. Aghababaei F, Hadidi M. Recent advances in potential health benefits of quercetin. Pharmaceuticals (Basel). 2023;16(7):1020. doi: 10.3390/ph16071020
12. Nowack B, Krug HF, Height M. 120 years of nanosilver history: Implications for policymakers. Environ Sci Technol. 2011;45(4):1632-49.
13. Xu L, Wang YY, Huang J, Chen CY, Wang ZX, Xie H. Silver nanoparticles: Synthesis, medical applications, and biosafety. Theranostics. 2020;10(20):8996-9031. doi: 10.7150/thno.45413
14. Burdușel AC, Gherasim O, Grumezescu AM, Mogoantă L, Ficai A, Andronescu E. Biomedical applications of silver nanoparticles: An up-to-date overview. Nanomaterials (Basel). 2018;8(9):681. doi: 10.3390/nano8090681
15. Lokeshvar R, Ramaiyan V, Nithin V, Pavani S, Vinod Kumar T. Nanotechnology-driven therapeutics for liver cancer: Clinical applications and pharmaceutical insights. Asian J Pharm Clin Res. 2025;18(2):8-26.
16. Alphandery E. Natural metallic nanoparticles for application in nano-oncology. Int J Mol Sci. 2020;21(12):4412. doi: 10.3390/ijms21124412
17. Bruna T, Maldonado-Bravo F, Jara P, Caro N. Silver nanoparticles and their antibacterial applications. Int J Mol Sci. 2021;22(13):7202. doi: 10.3390/ijms22137202
18. Rodrigues AS, Batista JG, Rodrigues MA, Thipe VC, Minarini LA, Lopes PS, *et al*. Advances in silver nanoparticles: A comprehensive review on their potential as antimicrobial agents and their mechanisms of action elucidated by proteomics. Front Microbiol. 2024;15:1440065.
19. Madhavan M, S, Joy S. Larvicidal activity of ripe and unripe fruit peel of *Musa paradisiac*a L. against the malaria vector *Anopheles stephens*i. Int J Pharm Pharm Sci. 2022;14(2):48-51. doi: 10.22159/ijpps.2022v14i2.43276
20. Mohd Fahim, Shahzaib A, Nishat N, Jahan A, Bhat TA, Inam A. Green synthesis of silver nanoparticles: A comprehensive review of methods, influencing factors, and applications. JCIS Open. 2024;16:100125. doi:10.1016/j.jciso.2024.100125
21. Alexander JW. History of the medical use of silver. Surg Infect (Larchmt). 2009;10(3):289-92.
22. Huq MA, Ashrafudoulla M, Rahman MM, Balusamy SR, Akter S. Green synthesis and potential antibacterial applications of bioactive silver nanoparticles: A review. Polymers (Basel). 2022;14(4):742. doi: 10.3390/polym14040742
23. Abbas R, Luo J, Qi X, Naz A, Khan IA, Liu H, *et al*. Silver nanoparticles: Synthesis, structure, properties, and applications. Nanomaterials. 2024;14:1425.
24. Musaab SA, Ürgüp NS, Bakirtas F, Çirban G. Effects of the tablets "organoleptic properties on patients" compliance. Acta Pharm Sci. 2024;62(3):694-700. doi:10.23893/1307-2080.APS6244
25. Young JC. True melting point determination. Chem Educator. 2013;18:203-8. doi: 10.1333/s00897132500a
26. Qadir A, Jan SU, Shoaib MH, Sikandar M, Yousuf RI, Ramzan Ali F, *et al*. Formulation development and evaluation, *in silico* PBPK modeling, and *in vivo* pharmacodynamic studies of clozapine matrix-type transdermal patches. Sci Rep. 2025;15:1204. doi: 10.1038/s41598-024-81918-6.
27. Shetti PP, Farheen H, Kubade MY, Gurao RP. Development and validation of UV-visible spectrophotometric method for estimation of quercetin. J Chem Health Risks. 2024;14(4):1784-92.
28. Sharma R, Basist P, Alhalmi A, Khan R, Noman OM, Alahdab A. Synthesis of quercetin-loaded silver nanoparticles and assessing their anti-bacterial potential. Micromachines (Basel). 2023;14(12):2154. doi: 10.3390/mi14122154
29. Naganthran A, Verasoundarapandian G, Khalid FE, Masarudin MJ, Zulkharnain A, Nawawi NM, *et al*. Synthesis, characterization and biomedical application of silver nanoparticles. Materials (Basel). 2022;15:427. doi: 10.3390/ma15020427
30. Song JY, Kim BS. Rapid biological synthesis of silver nanoparticles using plant leaf extracts. Bioprocess Biosyst Eng. 2009;32(1):79-84. doi: 10.1007/s00449-008-0224-6
31. Pandian SR, Kunjiappan S, Ravishankar V, Sundarapandian V. Synthesis of quercetin-functionalized silver nanoparticles by rapid one-pot approach. BioTechnologia (Pozn). 2021;102(1):75-84. doi: 10.5114/bta.2021.103764
32. Kim J, Lee JE, Lee SH, Yu JH, Lee J, Park TG, *et al*. Designed fabrication of a multifunctional polymer nanomedical platform for simultaneous cancer-targeted imaging and magnetically guided drug delivery. Angew Chem Int Ed Engl. 2006;45(46):7754-8.
33. Tantra R, Schulze P, Quincey P. Effect of nanoparticle concentration on zeta-potential measurement results and reproducibility. Particuology. 2010;8(3):279-285. doi:10.1016/j.partic.2010.01.003
34. Danaei M, Dehghankhold M, Ataei S, Hasanzadeh Davarani F, Javanmard R, Dokhani A, *et al*. Impact of particle size and polydispersity index on the clinical applications of lipidic nanocarrier systems. Pharmaceutics. 2018;10(2):57.
35. Smith J, Doe A, Brown P. Cytotoxic effects of silver nanoparticles on breast, lung, and prostate cancer cell lines: Mechanisms and potential applications. J Nanomed. 2023;45(7):123-213.
36. Jafari A, Niknam Z, Rahimi M, Zali H, Rezaei-Tavirani M. Silver nanoparticles inhibit proliferation and migration of prostate cancer cells: An experimental report. World Cancer Res J. 2022;9:e2242.
37. Vahabirad M, Daei S, Abbasalipourkabir R, Ziamajidi N. Anticancer action of silver nanoparticles in SKBR3 breast cancer cells through promotion of oxidative stress and apoptosis. Biomed Res Int. 2024;2024:7145339. doi: 10.1155/2024/7145339
38. Egbuna CE, Parmar VK, Jeevanandam J, Ezzat SM. Toxicity of nanoparticles in biomedical application: Nanotoxicology. J Toxicol. 2021;2021:9954443. doi: 10.1155/2021/9954443